ELSEVIER

Hydrometallurgy 37 (1995) 1–21

hydrometallurgy

Bacterial leaching of complex sulfide ore samples in bench-scale column reactors

Lasse Ahonen[a], Olli H. Tuovinen[b]

[a]*Geological Survey of Finland, FIN-02150 Espoo, Finland*
[b]*Department of Microbiology, Ohio State University, 484 West 12th Avenue, Columbus, OH 43210-1292, USA*

Received 17 August 1993; revised version accepted 4 February 1994

Abstract

Several variables were examined in column bioleaching of a complex sulfide ore material which contained chalcopyrite, pentlandite, pyrite, pyrrhotite and sphalerite as the main sulfide minerals. Samples were used with varying proportions of pyrrhotite, pyrite, quartzite (low acid consumption) and skarn (high acid consumption). The experiments were carried out using bench-scale column leaching reactors which were inoculated with acidophilic, Fe- and S-oxidizing bacteria, initially derived from the source mine water. Leaching rates in sterile controls were negligible. In inoculated columns new solid phases (covellite, jarosite, Fe(III) oxide and elemental sulfur) were formed. Acid consumption was highest under low pH and low redox potential conditions. The solubility of ferric iron was controlled by jarosite and an Fe(III) hydroxide (initially amorphous). The leaching rates of Co (from pyrite and pentlandite), Cu (chalcopyrite), and Zn (sphalerite) showed a tendency to increase with dissolved ferric iron concentration. The leaching of Ni (from pyrrhotite and pentlandite) did not correlate with the concentration of ferric iron in solution. Microscopic counts of bacteria in solution, deemed insufficient to represent total bacterial counts, showed a tendency to be higher at the lower pH and intermediate redox potential ranges. Trickle-leaching conditions yielded higher acid production and redox-potential values compared with flood leaching. The leaching rates of Co, Cu, Ni and Zn each responded differently to redox potential and pH regimes. The accelerating effect of a decreasing particle size on the metal leaching rates was amplified by low pH values.

1. Introduction

Industrial scale dump- and heap-leaching processes are especially suited for low-grade porphyry copper ores, in which primary copper minerals have been

0304-386X/95/$09.50
SSDI 0304-386X(94)00011-Q

partially altered to secondary sulfide and oxide minerals, which are readily amenable to oxidative and non-oxidative acid leaching. Acidophilic thiobacilli play an important role in these processes [1]. Other metals are dissolved from associated minerals in varying concentrations, but the current commercial heap-leaching processes are designed for Cu recovery. In the present report, the results are summarized from an extensive, laboratory-scale study dealing with the bacterial leaching of a complex Cu–Co–Zn ore.

The ore material was obtained from the Keretti mine, Outokumpu, eastern Finland. The geological setting and mineralogy of the deposit have been described by Peltola [2] and Koistinen [3]. Mining was carried out under ground. Upon the termination of mining activity, ore reserves remained which were not exploitable by conventional excavation techniques. An underground, in situ, leaching process was therefore considered as one of the possible alternative techniques. Several microbiological, chemical and physical factors influencing the leaching were included in the experimental plan. In the biological leaching process, the proper contact of ore material with the leach liquor is essential for fluxes of reactants and products, such as bacteria, dissolved gases (O_2 and CO_2), solubilized metals and sulfur species. In bench-scale studies, various percolator and column designs have been developed for studying the kinetics and optimization of biological leaching processes. Rate-controlling steps in copper heap-leaching systems have not been elucidated.

Ferric iron is an important oxidizing agent in the bacterial leaching of sulfide minerals. Soluble iron species are the main determinants of redox potential, with active iron-oxidizing bacteria (*Thiobacillus ferrooxidans*, *Leptospirillum ferrooxidans*) contributing to high Fe^{3+}/Fe^{2+} ratios. Precipitation of ferric iron in the leaching system may suppress the metal solubilization by preventing the contact between the leaching agent and the mineral. The solubility of iron is defined by the solution redox potential and pH. Thus, the optimization of these parameters may greatly improve the metal recovery.

The bacterial leaching process requires acidic conditions, the acidity often being autochthonously produced by the oxidation of pyrite and hydrolysis of ferric iron. The acid may, however, be neutralized in various acid-consuming reactions; for example, involving the leaching of carbonate minerals. Some silicate minerals also react in acid solution.

The solid/liquid contact area, which in low-porosity rocks is mainly a function of particle size of the material, is a major factor in determining the kinetics of the leaching reactions. Typical to leaching processes is their selectivity with respect to certain minerals or groups of minerals. The leaching effect is also able to penetrate into microfissures and micropores of the rock mass, thus reducing the need for energy consuming crushing and grinding operations. The optimization of a leaching process thus requires quantitative information on the effect of grain size, as well as on the propagation of the leaching effect inside the mineral grains.

As in all biochemical and chemical processes, the rates of leaching reactions are also temperature dependent. An experiment was also included in this study program to evaluate the effect of temperature on the bacterial leaching in column

reactors; the results have been presented elsewhere [4]. The characterization of the temperature effects of bioleaching on suboptimal temperatures was considered to be particularly important. An additional set of column leaching experiments was thus carried out to obtain more quantitative information on the temperature effects; the results have been reported [5].

In the leaching of complex sulfide ore, electrochemical interactions between sulfide minerals may play important role. Attention was thus also paid to the relative proportion of the different sulfide minerals, their mode of occurrence and textural relationships. The effect of silver addition was also tested in this set of long-term bacterial leaching experiments, as previously reported [6]. All these factors have a considerable interaction in active leaching processes and their relative effects should be taken into consideration in optimization studies.

2. Materials and methods

In the course of the study several samples from the ore, of different mixtures of the sulfide ore and gangue, were tested. Copper was present almost exclusively as chalcopyrite ($CuFeS_2$), zinc as sphalerite (ZnS), while cobalt was distributed in pentlandite [$(Co,Ni,Fe)_9S_8$] and pyrite (FeS_2). Nickel was associated with pentlandite and with pyrrhotite ($Fe_{1-x}S$). The average pyrite to pyrrhotite ratio in the ore is about 1:1, but spatial variation in their relative abundance in the ore occurs. Both pyrite-dominated and pyrrhotite-dominated samples were used in the experiments. In the leaching tests the sulfide ore samples were mixed with gangue material. In most experiments, the gangue material was carbonate and graphite-bearing siliceous metasediment, hereafter referred to as quartzite. In addition to quartzite, which is the immediate host rock of the ore, more effective acid-consuming material was also tested in the experiments. This material was a mixture of diopside- and tremolite-skarn, serpentinite and black schist, which also are typical in the mineralized rock association. The rock material was crushed and sieved in different size fractions. A summary of the experimental conditions and sample components in different experiments is presented in Table 1. The partial elemental composition of the ore samples is presented in Table 2.

The experiments were carried out with glass column reactors which, unless otherwise specified, contained 800 g of ore sample and 800 ml of leach solution (Table 1). The columns were 50 cm high with an internal diameter of 9 cm. The ore was placed on a fritted glass base which was raised from the bottom of the column. The leach solution was passed through the ore sample by gravity and recirculated through a side loop either by airlift or with a peristaltic pump. In two leaching experiments the column system (100×11 cm) comprised 12 kg ore material and 3 l of mineral salts solution.

The bacteria used in the column leaching experiments were derived by enrichment of mine water samples, using sulfide ore material from the mine site as the substrate. The leach solution contained 3.0 m*M* $(NH_4)_2SO_4$, 2.3 m*M* K_2HPO_4 and 1.6 m*M* $MgSO_4 \cdot 7H_2O$ in dilute sulfuric acid, with an initial pH of 2.5. Two

Table 1
Description of column leaching experiments

Column no.	Experimental parameter	Particle size (Ø, mm)	Pyrite/pyrrhotite ratio	Mixed component[b]	Ore sample[a]	Solid:liquid ratio (g/ml)
1	Enrichment					600/600
2	Enrichment					600/600
3	Continuous circulation of leach liquor	0.074–5	1:4	Q1	A	600/600
4	Periodic circulation of leach liquor	0.074–5	1:4	Q1	A	800/800
5	Aeration and removal of Fe(III) precipitate	0.074–5	1:4	Q1	A	800/800
6	Aeration and removal of Fe(III) precipitate	0.074–5	1:4	Q1	A	800/800
7	Continuous leaching, pH ≈2.5	0.074–5	1:4	Q1	A	800/800
8	Continuous leaching, pH ≈1.5	0.074–5	1:4	Q1	A	800/800
9	Uninoculated control	0.074–5	1:4	Q1	A	800/800
10	Inoculated column as reference to #9	0.074–5	1:4	Q1	A	800/800
11	Temperature, 4°C	1.68–5	1:4	Q2	B	800/800
12	Temperature, 10°C	1.68–5	1:4	Q2	B	800/800
13	Temperature, 19°C	1.68–5	1:4	Q2	B	800/800
14	Particle size	1.68–5	3:1	Q2	C	800/800
15	Particle size	5–10	3:1	Q2	D	800/800
16	Particle size	10–20	3:1	Q2	E	800/800
17	Particle size	1.68–5	3:1	G	F	800/800
18	Particle size	5–10	3:1	G	G	800/800
19	Particle size	10–20	3:1	G	H	800/800
20	Inoculated, pH≈2.5	1.68–5	3:1	Q3	I	800/800
21	Uninoculated, pH≈2.5	1.68–5	3:1	Q3	I	800/800
22	Inoculated, pH≈2.0	1.68–5	3:1	Q3	I	800/800
23	Uninoculated, pH≈2.0	1.68–5	3:1	Q3	I	800/800
24	Aeration and removal of Fe(III) precipitate	1.68–5	3:1	Q3	I	800/800
25	Fe(III) precipitation with NaOH	1.68–5	3:1	Q3	I	800/800
26	pH <2.5	1.68–5	3:1	Q3	I	800/800
27	pH <2.0	1.68–5	3:1	Q3	I	800/800
29	High-grade ore	1.68–5	1:1	–	J	400/800
30	Large column, 28°C	5–20	1:2	Q4	K	12,000/3,000
31	Large column, 28°C	5–20	1:2	Q4	K	12,000/3,000

[a] The chemical composition of the ore samples A–K is given in Table 2.
[b] Q1–Q4 = different quartzite samples (relatively low acid consumption); G = acid-consuming gangue (a mixture of serpentinite and skarn).

Table 2
Partial elemental analysis of ore samples used in column leaching experiments

Ore sample	Composition (%)					
	Cu	Zn	Ni	Co	Fe	S
A	0.29±0.04	0.32±0.03	0.16±0.02	0.056±0.003	11.6±0.3	8.5
B	0.23±0.05	0.31±0.12	0.17±0.01	0.058±0.008	12.2±1.4	7.4
C	0.59±0.26	0.08±0.01	0.11±0.04	0.077±0.020	9.6±1.3	10.7
D	0.52±0.28	0.08±0.02	0.12±0.04	0.057±0.015	8.2±1.5	7.6
E	0.68±0.31	0.12±0.06	0.12±0.02	0.087±0.037	10.3±2.6	7.8
F	0.042±0.13	0.04±0.01	0.11±0.01	0.049±0.013	7.8±1.3	6.5
G	0.50±0.15	0.18±0.10	0.10±0.02	0.056±0.014	8.8±1.3	6.5
H	1.2±1.2	1.16±0.15	0.08±0.02	0.079±0.026	11.5±1.8	7.3
I	0.64±0.28	0.07±0.02	0.10±0.02	0.079±0.029	8.3±2.2	10.1
J	6.15±0.25	0.43±0.02	0.08±0	0.61±0	38.1±2.1	36.0
K	1.0	0.50	0.30	0.10	10.5	9.1

The maximum deviation in results is given if three or more parallel analyses were available.

columns were initially set up for enrichment and operated for about 300 d. The cultures thus derived were used for inoculation in subsequent experiments. Unless otherwise stated, the column leaching experiments were carried out at 20±2°C. Sterile controls were included in three experimental sets.

During the experiments, samples (30 ml) were taken every 2 weeks for chemical analysis. Sample volumes were replaced with equivalent aliquots of mineral salts solution. Solution pH and redox-potential values were measured 2–3 times a week. Redox potential was measured with a Pt electrode using standard calomel electrode (SCE) as a reference. Loss of solution due to evaporation was estimated volumetrically and compensated for by adding sterile distilled water. The initial acid consumption was satisfied with sulfuric acid. Where necessary, sodium hydroxide was used to neutralize excessive acid production.

Dissolved metals were analyzed by atomic absorption spectrometry (AAS). The elemental composition of ore samples is based on averaged results obtained by AAS and by X-ray fluorescence spectrometry (XRF). Upon termination of the experiments, the solid residues were air dried and samples were taken for chemical analysis, X-ray diffraction (XRD) and ore microscopy. In some experiments, individual samples were taken for mineralogical examination during the active phase of leaching. The solid residues were dissolved in $HCl–HNO_3$ mixture and analyzed directly by AAS or indirectly by XRF. Total sulfur in solid residues was analyzed by combustion and IR detection (LECO IR 32H), S^0 by iodometric titration and sulfate indirectly by AAS determination of Ba after precipitation of $BaSO_4$. The chemical analyses were carried out by the analytical laboratory of Outokumpu Oy.

Leaching rates were calculated from the slopes of the metal dissolution curves for each data point. In order to reduce the effect of short-term changes and ana-

lytical errors on rate calculations, the metal dissolution curves were linearized with five data points, using the sum of least squares.

The concentration of dissolved Fe(III) was estimated on the basis of redox potential measurements, applying the Nernst equation. In these estimations, the speciation of the soluble complexes of ferric and ferrous iron was not systematically considered; only the species $FeSO_4^+$ was accounted for. Concentrations were taken to equal activities:

$$E = E_0 - \frac{RT}{n\mathcal{F}} \ln \frac{[FeSO_4^+]}{[Fe^{2+}][SO_4^{2-}]}$$

The thermodynamic data used in this work were obtained from the MINTEQ data base and from Brookins [7].

3. Results and discussion

3.1. General trends

A summary of metal dissolution rates in various experiments is given in Fig. 1. The leaching data are primarily based on experiments carried out at 20 ± 2°C, with the exception of one column leaching experiment each at 4 ± 1°C and 10 ± 1°C. The particle size encompassed three sizes in the range of 1.68–20 mm. Most of the data were obtained using a particle size fraction with a 1.68–5 mm diameter.

Long-term column leaching experiments lasted for about 2 yr, by which time more or less complete leaching of zinc was achieved. The yields of leaching amounted to about 50% for Ni and Co and <25% for Cu.

Leaching rates gradually decreased in the long-term leaching experiments (Fig.

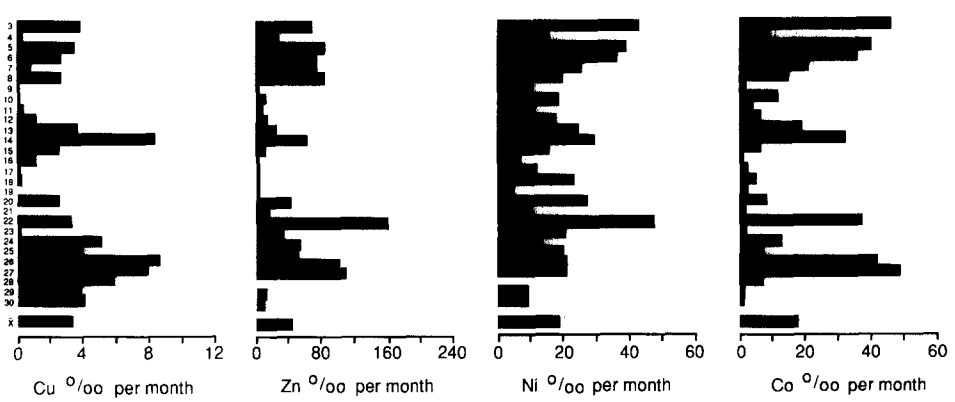

Fig. 1. Leaching rates of copper, zinc, nickel and cobalt in column leaching experiments, expressed as permil solubilization of each metal content per month. A total of 30 experiments were carried out, of which the first two were used only for culture enrichment purposes. The mean ($\bar{x}$) of leaching rates in experiments 3–30 is also given.

2). Because changes in leaching rates were evident even at low metal recoveries, this phenomenon cannot be entirely explained by the reduced amount of mineral material available. The decreased rates may be at least partially attributed to the formation of a product layer on the mineral surface which creates a diffusion barrier to the interfacial fluxes of reactants and products.

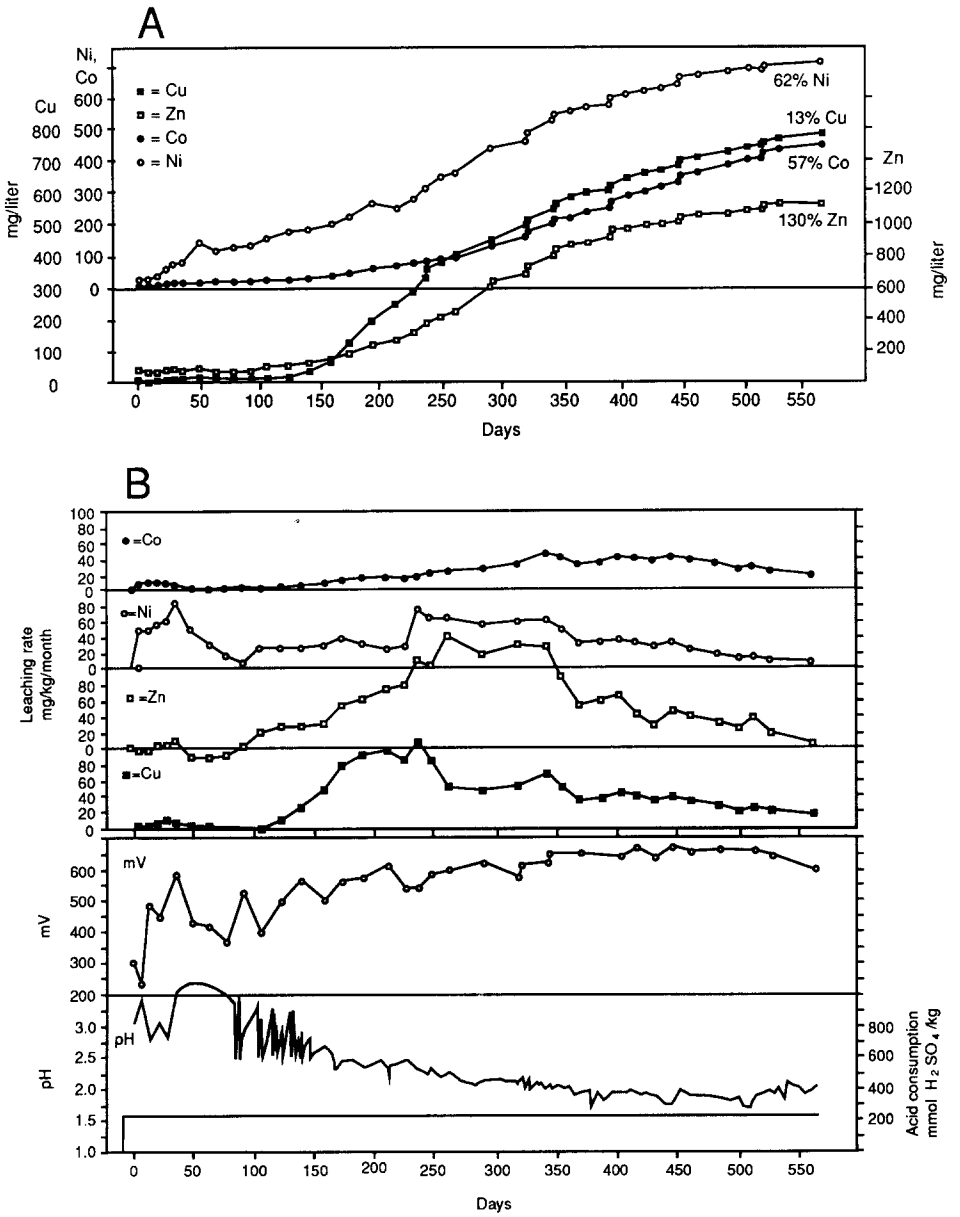

Fig. 2. Results of column leaching experiment no. 14. (a) Solubilization of copper, zinc, nickel and cobalt. (b) Changes in leaching rates, redox potential, pH and acid consumption.

The metal solubilization was simultaneously affected by several independent factors. Very low leaching rates were attributed to acid-consuming gangue material (experiments 17–19), low temperature (experiments 11 and 12), or a lack of bacterial catalysis (chemical controls, experiments 9, 21 and 23) (Fig. 1).

Nickel leaching rate was relatively high in the beginning of the experiments, decreasing strongly during the first half year (Fig. 2B). The maximum of the Ni leaching rate in the beginning of the experiments was usually accompanied by a minor increase in cobalt leaching rate. The main phase of cobalt leaching usually started later on. Solution analysis often showed zinc depletion in the beginning of the experiments, but subsequently the metal was readily solubilized. In many experiments soluble copper was virtually absent until pH adjustment to pH <2.5 started up the solubilization.

3.2. Mineralogical observations

Microscopic examination of the partially leached ore material revealed the common existence of Fe(III) oxide or oxyhydroxide coatings on mineral surfaces (Fig. 3). In experiments conducted at higher pH values (pH$\approx$3), Fe(III) precipitation in the particle interstices partially consolidated the material, suppressing its fluid permeability. Fine grained, loose precipitates were also frequently

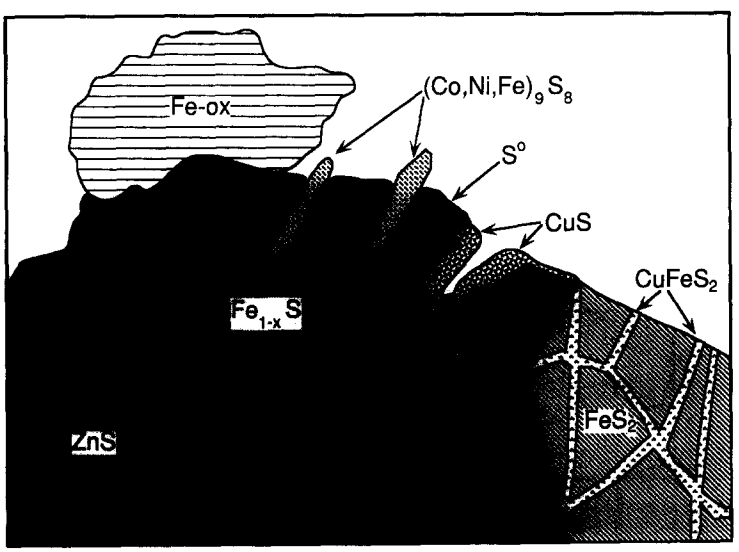

Fig. 3. Schematic diagram of mineralogical observations of leach residues. A compact Fe(III) oxide layer (*Fe-ox*) is illustrated as a layer on pyrrhotite ($Fe_{1-x}S$) surface. Pyrrhotite surfaces were characteristically covered by elemental sulfur (S^0) layer. Pentlandite inclusions [$(Co,Ni,Fe)_9S_8$] are shown relatively intact to indicate preferential dissolution of pyrrhotite. Pyrite (FeS_2) grains contained fissures with chalcopyrite ($CuFeS_2$) seams, both being relatively recalcitrant to bioleaching under these conditions. Shown also are covellite (CuS) precipitation on $Fe_{1-x}S$ and residual sphalerite (ZnS) in a fracture reaching inside $Fe_{1-x}S$.

observed on the surface of the leached material. At higher pH values the color of the precipitate was typically brown. At experiments conducted at pH values below pH 2.5, bright yellow precipitates were formed. The brown precipitate appeared to be amorphous in XRD analysis. The yellow precipitate was well crystallized and was identified by XRD as jarosite (general formula $X\mathrm{Fe_3(SO_4)_2(OH)_6}$, $X=\mathrm{K^+}$, $\mathrm{Na^+}$, $\mathrm{H_3O^+}$, $\mathrm{NH_4^+}$). Sodium jarosite was the main component in yellow precipitates. The major XRD reflections displayed spreading, which was attributed to the presence of potassium and hydronium jarosite. The chemical composition of some of the jarosite precipitates has been reported previously [6].

Precipitation of a secondary, Cu sulfide, covellite, on the surface of pyrrhotite was observed by microscopy (Fig. 3) and visual inspection. The presence of covellite was particularly pronounced when, in spite of the regular addition of sulfuric acid, the solution pH remained relatively high (pH 2.5–4), owing to the presence of alkaline gangue minerals. In some experiments the release of copper into solution was completely suppressed. Chemical analysis of leach solution samples suggested the precipitation of zinc in the course of the leaching but secondary zinc precipitates were not identified.

The solubility of iron monosulfide in an acid solution can be calculated from the following equation, which predicts that ferrous iron and hydrogen sulfide concentrations could exceed 1 m*M* concentration at pH 4.55:

$$\mathrm{FeS+2H^+ \rightleftarrows Fe^{2+}+H_2S} \quad \log K=3.1$$

Although thermodynamic properties of natural pyrrhotite may differ from the values used in this calculation, it can be concluded that non-oxidative dissolution of pyrrhotite, accompanied by the evolution of $\mathrm{H_2S}$, takes place in acid solutions [8].

The solubility of cupric sulfide is several orders of magnitude lower than that of iron sulfide and copper will precipitate if even minor amounts of hydrogen sulfide are present:

$$\mathrm{CuS+2H^+ \rightleftarrows Cu^{2+}+H_2S} \quad \log K=-16.0$$

The solubility of ZnS ($\log K=-4.6$) is several orders of magnitude lower than that of iron monosulfide. The exchange reaction between FeS and $\mathrm{Zn^{2+}}$ is also thermodynamically favorable:

$$\mathrm{FeS+Zn^{2+} \rightleftarrows ZnS+Fe^{2+}} \quad \log K=7.7$$

Covellite was observed to precipitate even at high redox potentials, if the solution pH was higher than about 2.5, and ferric iron was thus practically absent. In the presence of ferric iron, covellite formation seemed to be suppressed. This indicates that, in the absence of ferric iron, copper sulfide precipitation on the pyrrhotite surface is a faster process than the oxidation of soluble sulfide. Ferric iron is known to be an effective oxidizing agent for sulfide minerals but it may also oxidize soluble sulfide.

Elemental sulfur ($\mathrm{S^0}$) was observed in the chemical analysis of leach residues.

Elemental sulfur may be lost during preparation of polished sections for microscopic determinations. Partially leached pyrrhotite grains were frequently surrounded by dark rims (Fig. 3), containing unidentified powder material or casts of removed substance. The same texture was observed in shake flask experiments with pure pyrrhotite, with elemental sulfur as the main component in leach residue [9]. The formation of elemental sulfur is attributed to partial oxidation of pyrrhotite:

$$4Fe_{1-x}S + (3-3\times)O_2 + (12-12\times)H^+ \rightarrow (4-4\times)Fe^{3+} + 4S^0 + (6-6\times)H_2O$$

The leaching of pyrrhotite seemed to be controlled by crystallographic directions; preferentially advancing parallel to the direction of pentlandite lamellae. Comb-like textures were often observed. Pentlandite was observed to protrude on the partially leached pyrrhotite surface, indicating its relative resistance in comparison to pyrrhotite (Fig. 3). No significant differences in pyrrhotite leaching textures between the bacterial and solely chemical leaching were observed. Leaching of pyrite typically propagated along microfissures and grain boundaries. Solid residues were not found for pyrite leaching. Textures indicating pyrite leaching were not observed in the chemical controls.

In complex sulfide ore material, galvanic interactions between sulfide minerals may take place. Microscopic examinations [10] showed that in chemical controls chalcopyrite was preferentially leached with respect to pyrite when the two minerals were in contact. In bacterial leaching experiments, microscopic observations on polished specimens indicated that pyrite was more corroded than chalcopyrite. The leaching also seemed to propagate along the grain boundaries between pyrite and chalcopyrite grains.

3.3. Acid consumption

Active bacterial leaching necessitated periodic pH control, acid or base was added if the pH value deviated from the preferred pH range. Sulfuric acid was added during the pre-leaching phase and, even though acid production took place in the long-term experiments, the net process was acid-consuming in all tests. The acid demand varied depending on the experimental conditions; being highest under low pH and low redox potential conditions (Fig. 4). The acid addition averaged 43 g (0.44 mol) H_2SO_4/kg ore [91 g (0.93 mol) H_2SO_4/g Cu leached], including the initial pH adjustments. If estimated only for the pH and redox potential regime, where copper leaching was fastest (pH <2.5; redox potential >460 mV), the acid demand averaged 81 g H_2SO_4/g Cu leached.

Carbonate minerals are readily solubilized in acid solutions. The leaching of carbonate-rich gangue material, for example skarn, repeatedly increased the pH to values which were prohibitively high (pH >4) to the acid and bacterial dissolution of metals. Many silicate minerals are also partially solubilized in long-term acid leaching processes. The solubility of silica is low, and secondary sili-

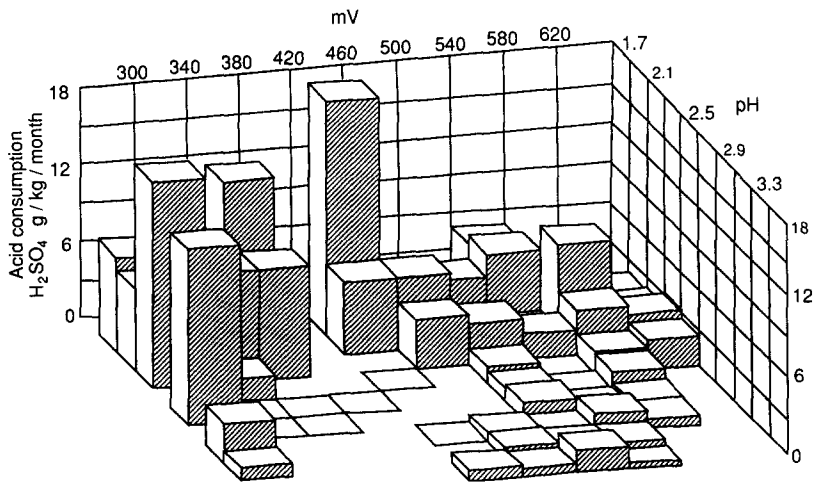

Fig. 4. Acid consumption as a function of pH and redox potential in column leaching experiments.

ceous precipitates may form. The dissolution and formation of solid phases of silicates have yet to be investigated for bacterial leaching processes. The leaching rates of silicates (Me_2SiO_4) are much lower than those of carbonates but their relative contribution to acid consumption is high, as is generically shown by the following equation:

$$Me_2SiO_4 + 4H^+ \rightleftarrows 2Me^{2+} + SiO_2 + 2H_2O$$

During the pre-leaching phase the smell of hydrogen sulfide was sometimes observed in the columns, indicating non-oxidative leaching of pyrrhotite. An increase in acid consumption coincided with an increase in redox potential and the concurrent leaching of nickel, suggesting partial oxidation of pyrrhotite.

3.4. Iron

A significant amount of iron was released from the sulfide minerals during the leaching process. It is evident that a major part of the dissolved iron was subsequently hydrolyzed and precipitated as ferric oxyhydroxide (used collectively for oxides, hydroxides and oxyhydroxides of ferric iron) but jarosites were also formed:

$$FeOOH + H_2O \rightleftarrows Fe^{3+} + 3OH^-$$

The solubility products of ferric oxyhydroxides reported vary from $10^{-36.6}$ to $10^{-43.7}$, depending on the nature of crystalline phase, on the degree of crystallinity and on the crystal size [11]. Poorly crystallized ferrihydrite and lepidocrocite are common products in the rapid hydrolysis of ferric iron. During the aging process these will be recrystallized and partially dehydrated, slowly converting to goethite (α-FeOOH; $\log K = -43$). The transformation to goethite is, however,

a slow process in acid solutions [12] and kinetic factors seem to favor the formation of jarosite. The solubility of Na-jarosite is defined by the following equation and the corresponding solubility product value was inferred from data published by Chapman et al. [13]:

$$NaFe_3(SO_4)_2(OH)_6 \rightleftarrows Na^+ + 3Fe^{3+} + 2SO_4^{2-} + 6OH^- \quad \log K = -89$$

A compilation of the dissolved iron concentration values as a function of measured pH in different experiments is presented in Fig. 5a. The sulfate concentrations in leaching solutions were not systematically analyzed. The total sulfate added for pH adjustment averaged 0.5 mol/l. It was also estimated that complete oxidation of sulfur in ore material would produce additional 0.5 mol sulfate/l. The concentration of pure sulfuric acid at pH 2 may be taken as representing the lowest limit of total soluble sulfate.

The respective ferric iron concentrations calculated from the total iron and redox potential data are shown in Fig. 5b. The solubilities of ferric iron precipitates in acid solutions are strongly affected by sulfate, which forms stable complexes with soluble ferric iron. Thermodynamic calculations based on these data suggested that the solubility of ferric iron was controlled by jarosite precipitation at pH <2.5 [8]. The concentration of dissolved ferric iron at pH >2.5 was negligible, presumably because of precipitation of Fe(III) oxyhydroxide or schwertmannite, a poorly crystalline Fe(III) oxyhydroxysulfate [14,15].

Soluble iron may act as an effective leaching agent whereas iron precipitates may suppress the dissolution processes. Fig. 6 shows the relationship between the amount of ferric iron in solution and the leaching rates of various metals. The average oxidation rates of Cu, Co and Zn increased when soluble iron was present in the leach solution at low concentrations; whereas the leaching of Ni did not exhibit any apparent correlation with the concentration of soluble iron.

The effect of iron precipitation on metal leaching rates was evaluated by comparing the concentration of total dissolved iron in solution with the estimated total amount of iron released from the ore material. The estimation was based on the known Co/Fe and Ni/Fe ratios in the minerals, and on the assumption that Co and Ni would not be incorporated into the precipitates. There appeared to be no relationship between the percentage fraction of iron in solution and the rate of leaching of either Cu, Ni, Co or Zn.

Attempts were also made to precipitate ferric iron by forced aeration of column effluents at pH >2.5. The increase in turbidity as a result of the forced aeration was negligible, suggesting that bacterial oxidation of iron was sufficient to maintain the iron in the oxidized form. In some experiments leach solutions were partially replaced periodically but no discernible effect could be seen on the leaching rates.

3.5. Bacteria

Bacterial leaching rates were clearly higher than the chemical leaching rates for the metals which were present in sulfide minerals in the ore samples. Chalcopyr-

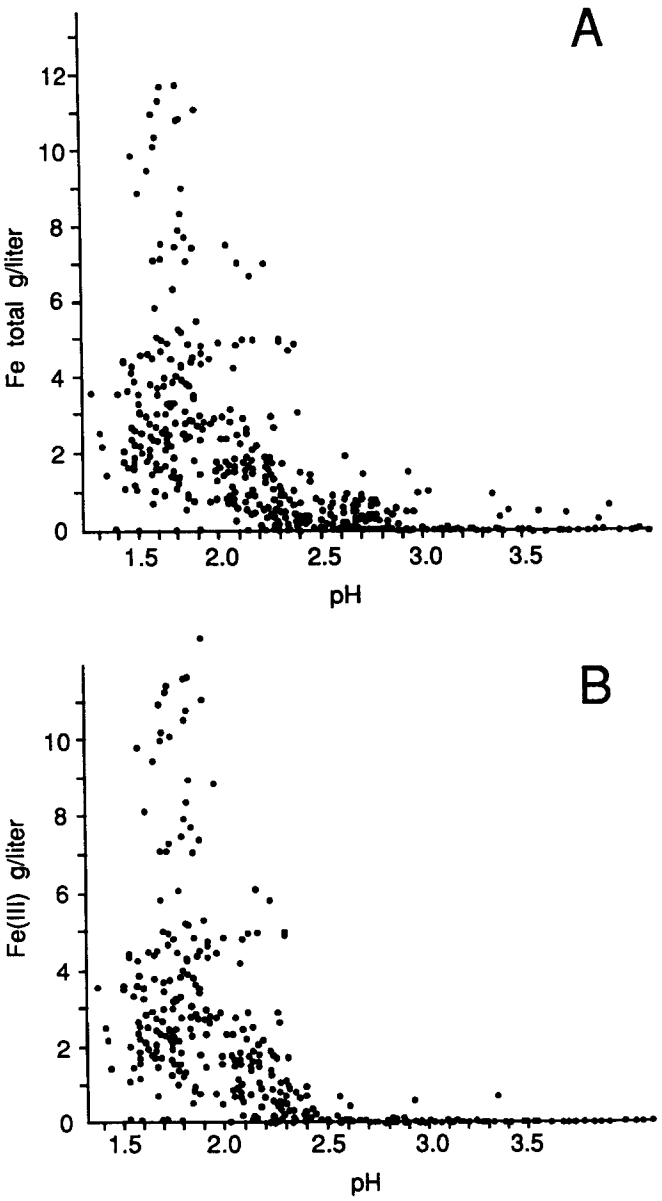

Fig. 5. Scatter diagram of (a) total dissolved iron concentration and (b) ferric iron concentration as a function of pH in column leaching experiments.

ite leaching was negligible without bacteria, as also was the solubilization of cobalt. Total iron reached higher concentrations with bacteria and the redox potential values were also higher, compared with the chemical controls. In the chemical controls, because of the lack of bacterial ferrous iron oxidation, redox potentials

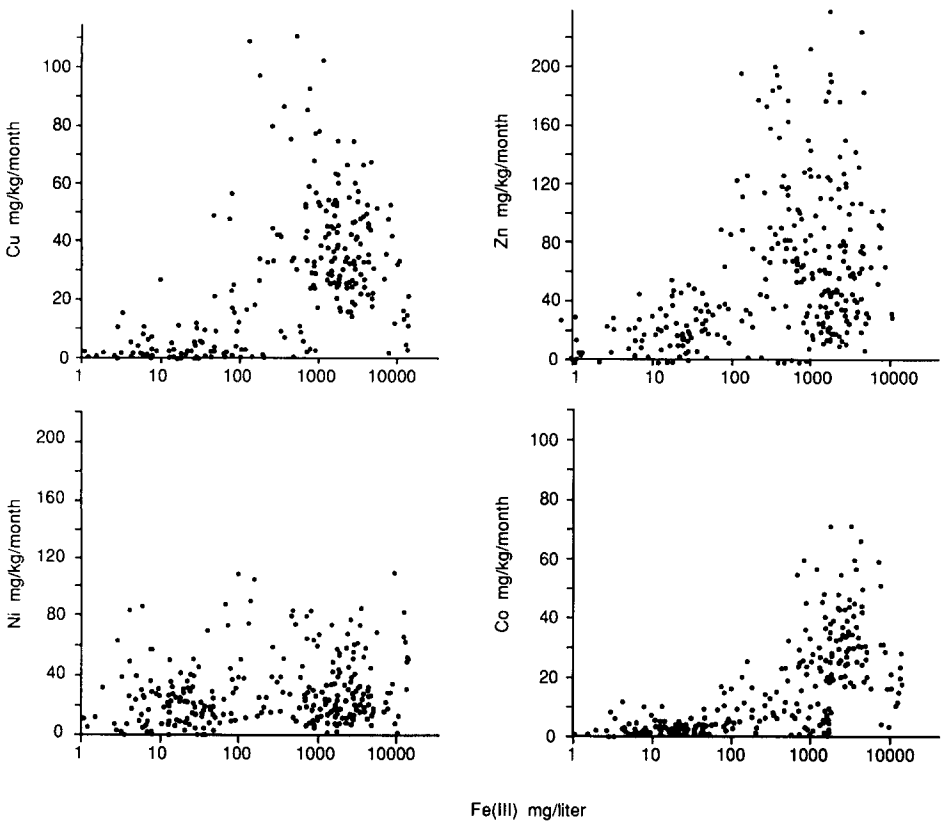

Fig. 6. Leaching rates of copper, zinc, nickel and cobalt as a function of ferric iron concentration in column leaching experiments.

remained low. Acid consumption was greatly reduced in the bacterial leach columns.

In some experiments attempts were made to enumerate bacteria by microscopic counts of effluent samples during column operation. It was a general trend with these results that higher bacterial counts were obtained at the lower pH range and at intermediate redox potential values (Fig. 7). This general tendency is in keeping with the dynamics of bioleaching whereby active bacteria account for the formation of oxidized chemical species in solution; the oxidation being coupled to growth, and thus to cell density. The bacterial counts are based only on free-swimming bacteria and no attempt was made to determine bacterial densities either qualitatively or quantitatively on mineral surfaces. At present, there is not sufficient information to evaluate the relative role of cell attachment in contributing to bacterial counts in active bioleaching systems.

3.6. Ore/liquid/air contact

In initial experiments, the daily column operation was based on either: (1) 2 h circulation followed by 22 h draining; or (2) continuous circulation of the leach

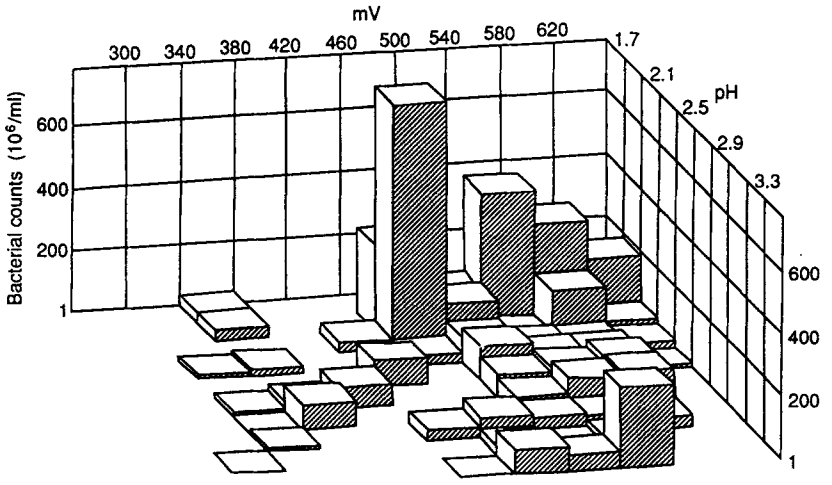

Fig. 7. Bacterial counts as a function of pH and redox potential in column leaching experiments.

solution while the ore was completely immersed and in full contact with the leach solution (flood leaching). The continuous circulation regime was found to be more effective.

Column design was subsequently modified to approximate trickle leaching conditions by raising the level of the fritted base in the column. This modification necessitated the insertion of a port below the base for pressure equilibration in the effluent holding zone. Larger columns, approximating trickle leaching conditions, were also set up to accommodate 12 kg ore samples and 3 l of leach solution.

A direct comparison with the two column designs, trickle leaching versus flooding (immersion), is difficult because of a number of other parameters that varied at the same time. If the comparison is based on the same ore material and approximately similar pH profiles under flood and trickle leaching conditions, the trickle leaching yielded approximately three times faster rates of copper and cobalt solubilization (experiments 20 and 26 at pH 2.5; experiments 22 and 27 at pH 2). More or less comparable leaching rates were obtained for nickel and zinc dissolution with the two techniques. Compared with trickle leaching, acid consumption was higher under flood leaching conditions. Trickle leaching consistently involved higher redox potential values (difference ≈ 100 mV) and the system became acid-producing. The flood leaching, on the other hand, displayed prolonged acid demand; evidence for the dissolution of acid-consuming minerals. Trickle leaching facilitates oxidative processes because of improved oxygen transfer conditions, whereas a flood leaching system gives better contact between mineral surface and water, thereby facilitating the leaching of pyrrhotite and non-oxidative dissolution of carbonate minerals.

3.7. Redox potential and pH

The redox potential and pH values during leaching experiments varied for many reasons. Prior to inoculation, the columns were pre-leached with sulfuric acid (pH≈2) in order to neutralize the alkaline components of the ore material. Bacterial oxidation of ferrous iron to the ferric form usually took place during the first weeks of the experiment, increasing the redox potential from initial values of ≈300–400 mV to >500 mV. The increase in redox potential was usually accompanied by an increase in acid consumption and in metal solubilization. While the redox conditions were mainly controlled by bacterial activity and oxygen supply, the solution pH was usually maintained at predetermined levels.

Fig. 8 illustrates the general effects of pH and redox potential on the leaching of various metals. The average rates of solubilization of Co and Cu were highest at high redox potential and low pH values, while the leaching of Ni displayed practically no pH or redox potential dependence. The average copper leaching rate increased rapidly at pH <2.5 and at redox potential values >500 mV. Reasonable Zn leaching rates were obtained at lower redox potential values (≈400–500 mV) and they were also less dependent on solution pH. Compared with the other metals, the rate of cobalt leaching displayed a more apparent dependence on the change in pH and redox potential.

The general trends observed here can be attributed to the electrochemical nature of the respective sulfide minerals. The sulfide minerals studied here are thermodynamically unstable in oxidative conditions. A generalized half-cell reaction describing the complete oxidation and leaching of a sulfide mineral (MeS) can be written as:

$$MeS + 4H_2O \rightleftarrows Me^{2+} + SO_4^{2-} + 8e^- + 8H^+$$

Assuming activities of [Cu]=0.01, [Zn]=0.01, [Fe]=0.1, $[SO_4^{2-}]$=0.1 and pH=2, the following thermodynamic equilibrium potentials (SCE) were calculated from the respective equilibrium constant (K) values: chalcopyrite=273 mV; pyrite=267 mV; sphalerite=232 mV; and pyrrhotite=167 mV. The solution redox potential values measured in the experiments clearly exceeded the calculated equilibrium potentials.

An updated compilation of measured sulfide mineral single electrode potentials is given by Rossi [1]. Values from 500 to 600 mV (standard hydrogen scale, corresponding to about 250–350 mV SCE) have been measured for pyrite, with slightly lower values for chalcopyrite. This is in agreement with the observations that galvanic coupling between pyrite and chalcopyrite promotes chalcopyrite oxidation [16,17]. In the present experiments, galvanic effects between pyrite and chalcopyrite were clearly demonstrated with chemical controls, in which redox potentials were typically low. A major source of Co in this ore was pyrite, which has the highest electrode potential in the electrochemical series of the common sulfide minerals [1,18]. In bacterially catalyzed leaching, when redox potential and ferric iron concentrations were high, rapid pyrite leaching appeared to pre-

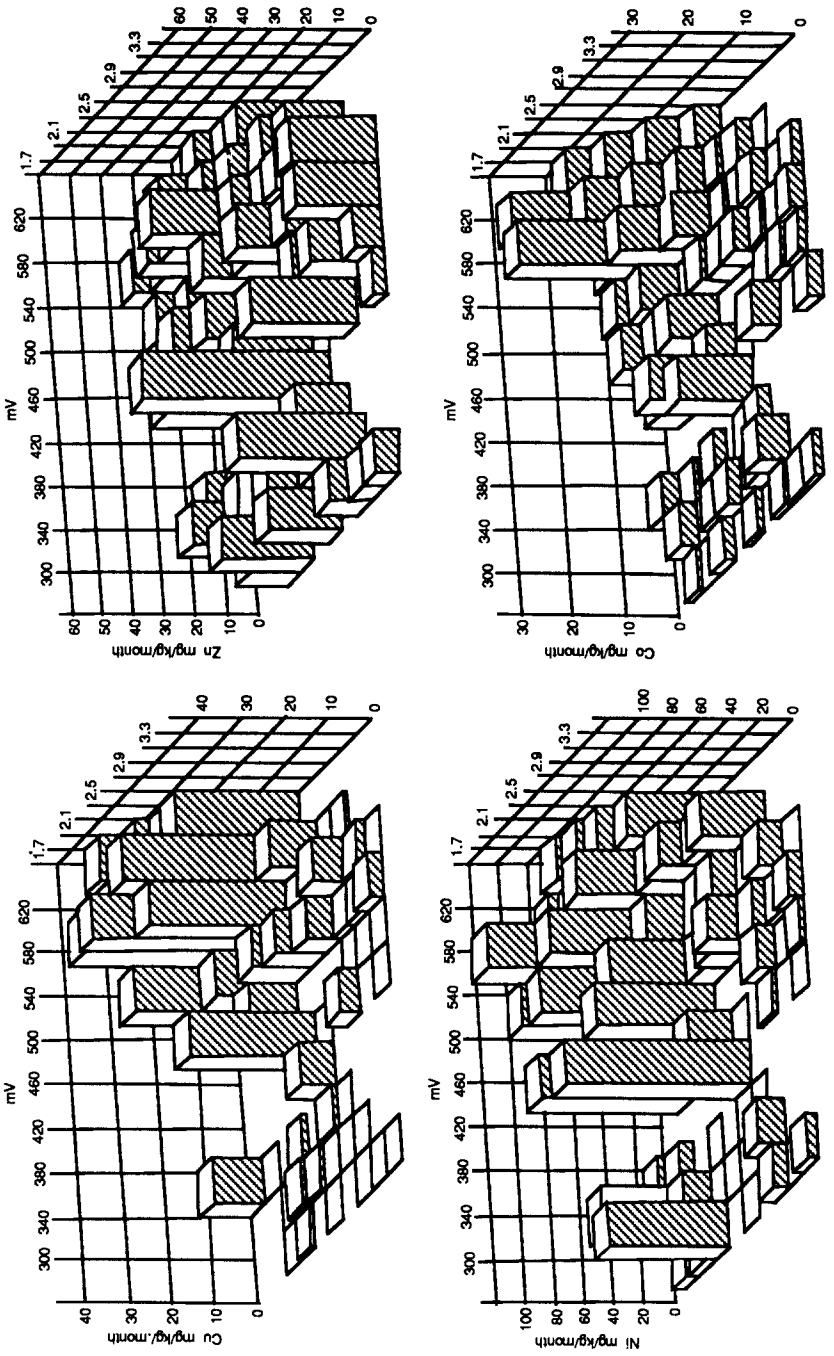

Fig. 8. Leaching rates of copper, zinc, nickel and cobalt as a function of pH and redox potential in column leaching experiments.

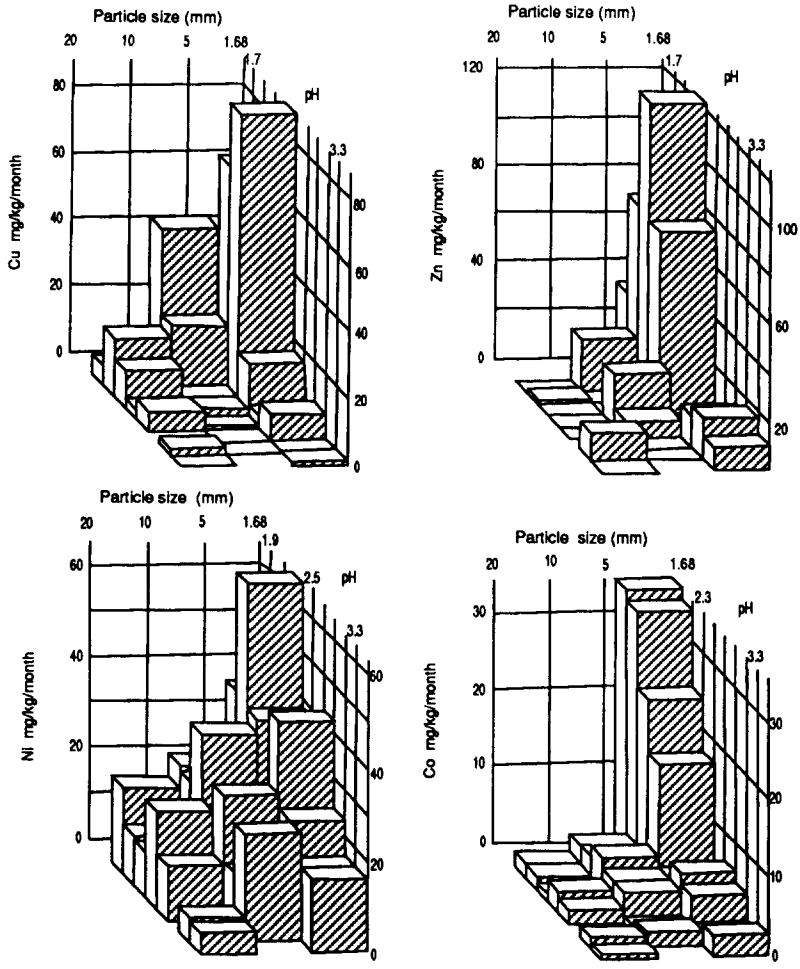

Fig. 9. Leaching rates of copper, zinc, nickel and cobalt as a function of particle size fraction in column leaching experiments.

dominate. Pyrrhotite leaching did not show any dependence on the redox potential, suggesting that the rate-determining step is not a redox reaction.

Pyrite and chalcopyrite have higher electrode potentials and are more recalcitrant than sphalerite, pyrrhotite and pentlandite. Pyrrhotite (the main source of Ni in this ore) has a low electrode potential and is more readily dissolved than $CuFeS_2$ and FeS_2, as is apparent from the broad pH–redox potential range where nickel dissolution took place.

The electrochemical control of leaching in these column experiments is obscured by several factors. For example, the minerals may mask each other in ore particles, in which case sequential chemical leaching may override galvanic effects. Bacterial distribution and indiscriminate oxidative attack of metal sulfides

may also obscure effects attributable to the leaching of minerals in an electrochemical series.

3.9. Particle size

Fig. 9 shows the effect of particle size on metal leaching rates, summarized from column leaching experiments 14–16 and 17–19. The leaching rates for all metals increased with a smaller particle size fraction and this effect was amplified at decreasing pH values. This trend is attributed to the increased solubility of Fe^{3+} and higher redox potential at low pH values which, together with a geometric increase in the available surface area, cause the positive rate effect. Copper and nickel leaching rates approximately doubled when the particle diameter was decreased from 5–10 mm to 1.68–5 mm. Concurrent zinc dissolution displayed a five- to seven-fold increase in the respective rate and that of Co was accelerated over ten-fold.

4. Concluding remarks

The results demonstrate that there are several interacting parameters in the bacterial leaching of sulfide minerals. Low leaching rates were typical with acid-consuming gangue material, at low temperatures, or in the absence of bacterial catalysis. Hydrogen sulfide formation was evident; suggesting non-oxidative leaching, which was attributed to the presence of pyrrhotite. Owing to the toxicity of H_2S, the non-oxidative leaching in the initial stages may be detrimental to bacterial activity. Active leaching of pyrrhotite, most important in the initial phase, was a net acid-consuming reaction. When pyrite oxidation was the major oxidative reaction, the leaching of the ore material became a net acid-producing phase. The length of the acid-consuming and acid-producing phases during the leaching was controlled by the relative amount of sulfide minerals, the temperature and the presence of gangue minerals.

Ferric iron is a key component in sulfide mineral leaching. It is important to ensure the bacterial regeneration of ferric iron, otherwise the leaching becomes non-oxidative and occurs at a low redox potential level. With little or no bacterial activity, ferrous iron predominates as the redox species and oxidative leaching is almost negligible. Of the various sulfide minerals present in the ore, pyrrhotite leaching was the least sensitive to low redox potential. However, for all sulfide minerals present in this ore, the data emphasize that the fastest leaching rates are achieved under oxidized conditions (high redox potential) and at low pH values, where a considerable portion of ferric iron remains in solution; that is, under conditions where bacterial activity is responsible for oxidative leaching of sulfide minerals. The relationships between leaching rates and pH, redox potential and ferric iron in solution, which vary for each discreet mineral, suggest that there is no uniform mechanism of mineral dissolution in biological leaching. The apparent lack of a universal mechanism to explain the biological leaching of sulfide

minerals in this work warrants fundamental studies of biological and electrochemical mechanisms to understand, optimize and develop models for biological leaching processes.

Acknowledgements

The experimental work was carried out in the Department of Microbiology, University of Helsinki. We are grateful to Ms. Paula Hiltunen for her skillful participation in the planning and experimental phases of the work, Ms. Sinikka Pahkala for technical assistance and Dr. Martti Lehtinen (Geological Museum, University of Helsinki) for XRD analysis of leach residues. We appreciate the analytical services and the collaboration with several experts from Outokumpu Oy during the experimental phase of the project. The work was funded by the Ministry of Trade and Industry (Finland). Additional financial support was received from Outokumpu Research Oy and the Nordisk Industrifond.

References

[1] Rossi, G., Biohydrometallurgy. McGraw-Hill, Hamburg (1990).
[2] Peltola, E., Origin of Precambrian copper sulfides of the Outokumpu district, Finland. Econ. Geol., 73 (1978): 461–477.
[3] Koistinen, T.J., Structural evolution of an early Proterozoic strata-bound Cu–Co–Zn deposit, Outokumpu, Finland. Trans. R. Soc. Edinburgh Earth Sci., 72 (1981): 115–158.
[4] Ahonen, L. and Tuovinen, O.H., Temperature effects on the microbiological leaching of complex sulfide ore material in percolators containing chalcopyrite, sphalerite, pentlandite, and pyrrhotite as main minerals. Biotechnol. Lett., 11 (1989): 331–336.
[5] Ahonen, L. and Tuovinen, O.H., Bacterial oxidation of sulfide minerals in column leaching experiments at suboptimal temperatures. Appl. Environ. Microbiol., 58 (1992): 600–606.
[6] Ahonen, L. and Tuovinen, O.H., Silver catalysis of the bacterial leaching of chalcopyrite-containing ore material in column reactors. Miner. Eng., 3 (1990): 437–445.
[7] Brookins, D.G., Eh–pH Diagrams for Geochemistry. Springer, Berlin (1988).
[8] Ahonen, L. and Tuovinen, O.H., Solid-phase alteration and iron transformation in column bioleaching of a complex sulfide ore. In: C.N. Alpers and D.W. Blowes (Editors), Environmental Geochemistry of Sulfide Oxidation. Am. Chem. Soc., Washington, D.C. (1994), pp. 79–89.
[9] Ahonen, L., Hiltunen, P. and Tuovinen, O.H., The role of pyrrhotite and pyrite in the bacterial leaching of chalcopyrite. In: R.W. Lawrence, R.M.R. Branion and H.G. Ebner (Editors), Fundamental and Applied Biohydrometallurgy. Elsevier, Amsterdam (1986), pp. 13–22.
[10] Ahonen, L. and Tuovinen, O.H., Alterations in surfaces and textures of minerals during the bacterial leaching of a complex sulfide ore. Geomicrobiol. J., 10 (1993): 207–217.
[11] Macalady, D.L., Langmuir, D., Grundl, T. and Elzerman, A., Use of model-generated Fe^{3+} ion activities to compute Eh and ferric oxyhydroxide solubilities in anaerobic systems. In: D.C. Melchior and R.L. Bassett (Editors), Chemical Modeling of Aqueous Systems II. Am. Chem. Soc., Washington, D.C. (1990), pp. 350–367.
[12] Schwertmann, U. and Murad, E., Effect of pH on the formation of goethite and hematite from ferrihydrite. Clays Clay Miner., 31 (1983): 277–284.
[13] Chapman, B.M., Jones, D.R. and Jung, R.F., Processes controlling metal ion attenuation in acid mine drainage streams. Geochim. Cosmochim. Acta, 47 (1983): 1957–1973.

[14] Bhatti, T.M., Bigham, J.M., Carlson, L. and Tuovinen, O.H., Mineral products of pyrrhotite oxidation by *Thiobacillus ferrooxidans*. Appl. Environ. Microbiol., 59 (1993): 1984–1990.
[15] Bigham, J.M., Carlson, L. and Murad, E., Schwertmannite, a new iron oxyhydroxysulfate from Pyhäsalmi, Finland, and other localities. Miner. Mag. (1994), in press.
[16] Berry, V.K., Murr, L.E. and Hiskey, J.B., Galvanic interactions between chalcopyrite and pyrite during bacterial leaching of low grade wastes. Hydrometallurgy, 3 (1978): 309–326.
[17] Mehta, A.P. and Murr, L.E., Fundamental studies of the contribution of galvanic interaction to acid-bacterial leaching of mixed metal sulfides. Hydrometallurgy, 9 (1983): 235–256.
[18] Natarajan, K.A., Electrochemical aspects of bioleaching of base-metal sulfides. In: H.L. Ehrlich and C.L. Brierley (Editors), Microbial Mineral Recovery. McGraw-Hill, New York (1990), pp. 79–106.